Real-time imaging of the intracellular glutathione redox potential

Marcus Gutscher[1], Anne-Laure Pauleau[1], Laurent Marty[2], Thorsten Brach[2], Guido H Wabnitz[3], Yvonne Samstag[3], Andreas J Meyer[2] & Tobias P Dick[1]

Dynamic analysis of redox-based processes in living cells is now restricted by the lack of appropriate redox biosensors. Conventional redox-sensitive GFPs (roGFPs) are limited by undefined specificity and slow response to changes in redox potential. In this study we demonstrate that the fusion of human glutaredoxin-1 (Grx1) to roGFP2 facilitates specific real-time equilibration between the sensor protein and the glutathione redox couple. The Grx1-roGFP2 fusion protein allowed dynamic live imaging of the glutathione redox potential (E_{GSH}) in different cellular compartments with high sensitivity and temporal resolution. The biosensor detected nanomolar changes in oxidized glutathione (GSSG) against a backdrop of millimolar reduced glutathione (GSH) on a scale of seconds to minutes. It facilitated the observation of redox changes associated with growth factor availability, cell density, mitochondrial depolarization, respiratory burst activity and immune receptor stimulation.

Intracellular redox changes accompany major transitions in the life cycle of metazoan cells, such as proliferation, differentiation, senescence and death[1–4]. Redox changes can be either short-lived, as exemplified by transient and localized production of reactive oxygen species (ROS) in the course of normal growth factor signaling[5], or long-lived, as observed in the case of cellular senescence[6,7]. Pro-oxidative redox states can also be inflicted by the activation of host defense, notably inflammation[8], as well as abiotic factors. Elevated and prolonged oxidative stress has been associated with various age-related pathophysiologies, including neurodegenerative, malignant and cardiovascular disorders. Mounting evidence suggests that oxidative processes can have a causal role in disease initiation or progression[9]. Although there appears to exist a broad consensus that pro-oxidative redox changes are important in health and disease, their labile and context-dependent nature has made their undisturbed observation notoriously difficult.

Recent evidence suggests that informative measurements of cellular redox states might be more challenging than previously realized. Cells harbor several redox systems, which appear to be kinetically controlled and not in equilibrium with each other[10]. They have distinct regulatory functions and are themselves subject to independent regulation. Measurement of one redox pair does not necessarily inform about the state of other redox couples[11]. Moreover, the spatiotemporal pattern of intracellular redox changes may be highly nonuniform between and within cellular compartments[12,13]. Understanding the relevance and specificity of redox changes will require nondisruptive measurements with specificity for defined redox pairs and considerable spatiotemporal resolution.

The lack of tools for measuring the status of defined intracellular redox couples has been a profound limitation for basic research. Conventional approaches either lack well-defined specificity or disrupt cellular integrity. For example, redox-sensitive fluorescent dyes, frequently used to detect oxidant generation within cells, interact with multiple oxidants and may even promote artificial ROS formation[14]. Customary redox measurements of glutathione and thioredoxin, though specific for the respective redox couple, require cell lysis and analytical separation procedures, making measurements prone to artifacts.

Genetically encoded biosensors promise to overcome the limitations of conventional redox measurements. Most recently, the H_2O_2-sensing properties of the bacterial protein OxyR had been exploited to develop HyPer, a yellow fluorescent protein (YFP)-based biosensor for intracellular hydrogen peroxide[15]. Before it, others[16,17] developed redox-sensitive fluorescent proteins by inserting an artificial dithiol-disulfide pair into the structures of YFP and GFP, respectively. A major advantage of the latter (called redox-sensitive GFPs or roGFPs) is that they are ratiometric by excitation, thus minimizing measurement errors resulting from variable concentration or photobleaching. However, endogenously expressed roGFPs do not appear to respond to physiologically relevant redox signals in animal cells[12]. It has been concluded that the usefulness of existing roGFPs is limited by their slow response to changes in redox potential. Moreover, it has remained unclear which endogenous cellular redox systems actually interact with roGFPs.

We reasoned that conventional roGFPs might be oblivious to most endogenous redox changes because their equilibration with cellular redox systems is too slow and unselective. Following this consideration, we explored the concept of equipping the biosensor

[1]Redox Regulation Research Group, German Cancer Research Center (DKFZ/A160), Im Neuenheimer Feld 280, D-69120 Heidelberg, Germany. [2]Heidelberg Institute of Plant Sciences, University of Heidelberg, Im Neuenheimer Feld 360, D-69120 Heidelberg, Germany. [3]Institute of Immunology, University of Heidelberg, Im Neuenheimer Feld 305, D-69120 Heidelberg, Germany. Correspondence should be addressed to T.P.D. (t.dick@dkfz.de).

RECEIVED 15 JANUARY; ACCEPTED 7 APRIL; PUBLISHED ONLINE 11 MAY 2008; DOI:10.1038/NMETH.1212

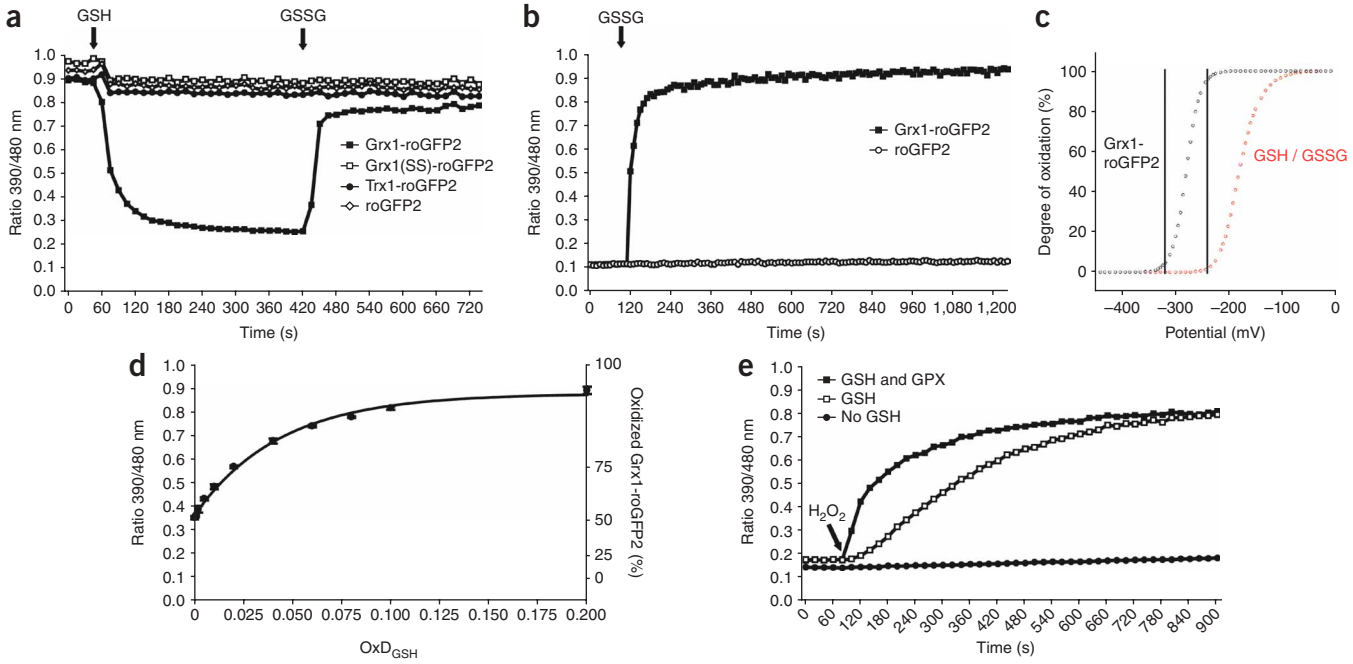

Figure 1 | Grx1 dynamically catalyzes rapid redox equilibration between glutathione and roGFP2. (**a**) Oxidized Grx1-roGFP2, Grx1(SS)-roGFP2, Trx1-roGFP2 and roGFP2 were reduced by injection of 15 mM GSH after 45 s and oxidized with 100 μM GSSG after 7 min. Incomplete reduction of Grx1-roGFP2 by GSH is due to the presence of trace amounts of GSSG. (**b**) Oxidation of reduced Grx1-roGFP2 and roGFP2 with 10 μM GSSG, injected after 110 s. (**c**) Nernst relationship between redox potential, OxD_{roGFP2} and OxD_{GSH} (at 10 mM total glutathione). The vertical lines are visual guides to indicate that within the physiological range small changes in OxD_{GSH} lead to large changes in OxD_{roGFP2}. (**d**) Grx1-roGFP2 was incubated with glutathione solutions (20 mM total) containing increasing fractions of GSSG. The indicated OxD_{GSH} is calculated from the amount of GSSG supplied to the redox buffer and does not take into account traces of GSSG already present in the GSH preparation. (**e**) After 75 s, 100 μM H_2O_2 was injected into a solution of reduced Grx1-roGFP2, in buffer alone, with 5 mM fully reduced GSH with or without 0.1 units of glutathione peroxidase (GPX). To remove residual GSSG from the GSH solution before use, the least amount of NADPH (30 μM) required to achieve near-complete reduction by 0.1 μM glutathione reductase was added. Data are representative of two (**a**,**d**,**e**) or three (**b**) experiments.

with an enzyme to specifically catalyze the equilibration between the redox pair of interest, reduced glutathione (GSH) and oxidized glutathione (GSSG), and the reporting redox couple ($roGFP2_{red}$ and $roGFP2_{ox}$). Here we demonstrate that the fusion of roGFP2 and human glutaredoxin-1 (Grx1) allows dynamic live imaging of intracellular glutathione redox potential, E_{GSH}, with unprecedented sensitivity and temporal resolution. The sensor detected both short- and long-lived deflections of endogenous E_{GSH} and facilitated the observation of physiologically relevant redox-based signals.

RESULTS

Grx1 catalyzes equilibration between glutathione and roGFP2

To enforce rapid and specific equilibration, we fused either human Grx1 or thioredoxin-1 (Trx1) to the N terminus of roGFP2, linked by a 30-amino-acid spacer, $(Gly\text{-}Gly\text{-}Ser\text{-}Gly\text{-}Gly)_6$, to allow for flexible interactions between the linked entities. For control experiments, we generated a catalytically inactive Grx1 fusion protein by replacing active site cysteines with serines (Grx1(ss)-roGFP2). We first confirmed that the fusion of either Grx1 or Trx1 to roGFP2 did not interfere with its intrinsic redox-sensing and ratiometric properties (**Supplementary Fig. 1** online). We also verified that the fluorescence excitation spectrum was not influenced by the fusion (data not shown) and that the emission ratio of the sensor constructs was insensitive to pH changes between 5.5 and 8.5 (**Supplementary Fig. 2** online).

Next we examined the response of unfused and fused roGFP2 to consecutive exposure to reduced and oxidized glutathione. Only the catalytically active Grx1-roGFP2 fusion protein responded to glutathione injections, thus demonstrating that Grx1, but not Trx1, confers dynamic responsiveness to the GSH/GSSG redox state (**Fig. 1a**). To estimate the kinetic advantage mediated by fused Grx1, we measured the rate of GSSG-mediated oxidation of Grx1-coupled and uncoupled roGFP2 at various GSSG concentrations, as exemplified by the response to 10 μM GSSG (**Fig. 1b** and see **Supplementary Fig. 3** online for corresponding emission intensity measurements). Kinetic analysis revealed that the oxidation of Grx1-roGFP2 by GSSG is at least 100,000 times faster as compared to uncoupled roGFP2.

As the midpoint redox potential of roGFP2 (–280 mV[18]) is more reducing compared to that of glutathione at physiological concentrations (ranging from –151 mV at 1 mM to –181 mV at 10 mM), we anticipated that even a small increase in the amount of glutathione oxidation (OxD_{GSH}, for a mathematical definition see **Supplementary Methods** online) within a highly reduced glutathione pool should give rise to a large and disproportionate degree of sensor oxidation (OxD_{roGFP2}). Calculation of corresponding Nernst potentials (see **Supplementary Methods**) confirmed that the redox sensor is expected to be highly sensitive to glutathione oxidation because the physiologically relevant potential range between –320 mV and –240 mV is covered by only minor changes in OxD_{GSH} (**Fig. 1c**). To verify the predicted sensitivity of

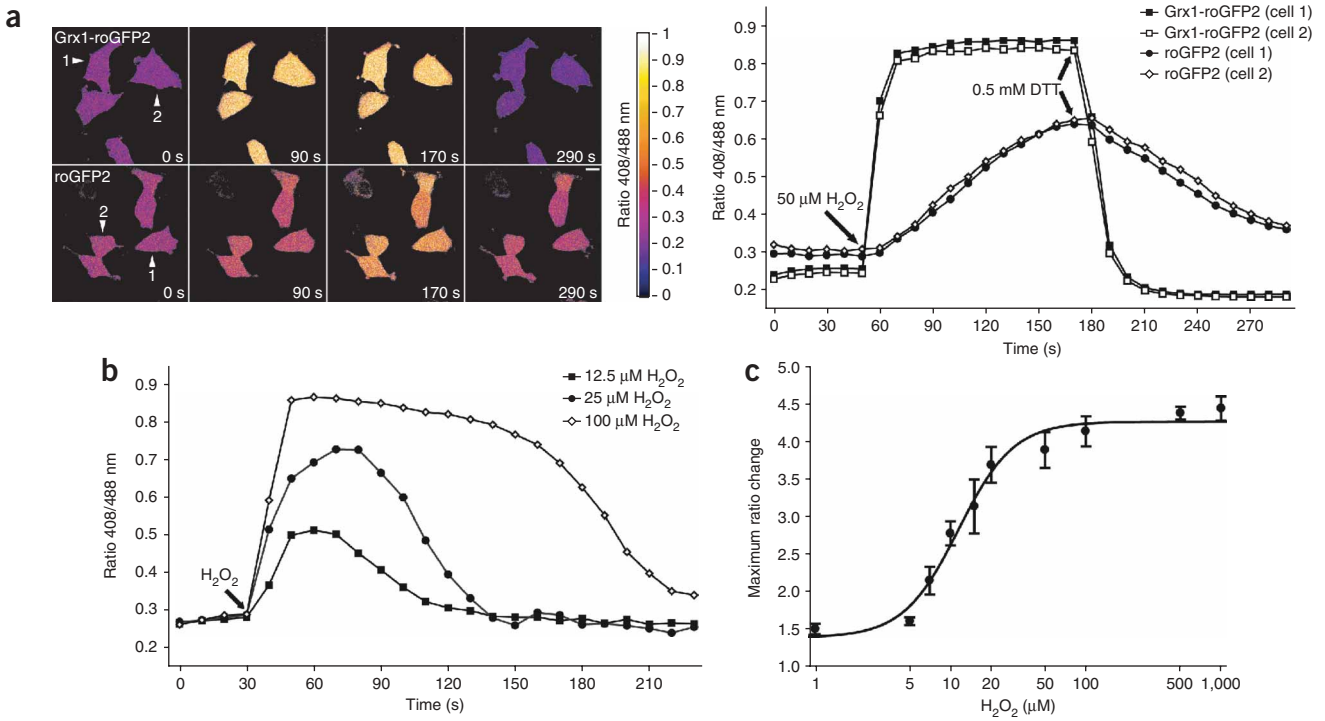

Figure 2 | Grx1-roGFP2 fusion protein allows live imaging of rapid intracellular redox changes. (**a**) HeLa cells expressing Grx1-roGFP2 or roGFP2 were excited with 408 and 488 nm lasers, and the ratio of emissions in the green channel (500–530 nm) was calculated. After 50 s, cells were treated with 50 μM H_2O_2 followed by addition of 500 μM DTT 2 min later. False-color ratio pictures of the cells at indicated time points exemplify the kinetic difference between Grx1-roGFP2 and roGFP2 (left). Scale bar, 10 μm. In each experiment, the ratio was quantified for two individual cells (arrowheads) and plotted against time (right). (**b**) Grx1-roGFP2–expressing HeLa cells were treated with the indicated amounts of H_2O_2 30 s after starting the measurement and the ratiometric sensor response was measured. (**c**) Based on experiments similar to those in **b**, the maximal ratio change of cells expressing Grx1-roGFP2 was plotted against H_2O_2 concentration. For each point in the graph at least 6 cells from 3 different experiments were analyzed. A ratio value of 1.0 represents the fully reduced (DTT-treated) state. Error bars represent s.d. from the mean. Data are representative of three experiments.

the sensor, we measured the response of the Grx1-roGFP2 sensor at various OxD_{GSH} and obtained a curve consistent with theoretical expectations (**Fig. 1d**). Of note, commercially available GSH contained traces of GSSG (typically corresponding to an OxD_{GSH} between 0.0015 and 0.002), which led to substantial sensor oxidation, for example, 50% in a 20 mM GSH solution (**Fig. 1d**) or 96% in a 1 mM GSH solution (data not shown). To verify that sensor oxidation in freshly prepared GSH solutions is due to trace amounts of GSSG, we treated GSH solutions with glutathione reductase and NADPH, thus clamping Grx1-roGFP2 in the fully reduced state, corresponding to a E_{GSH} below –320 mV (**Supplementary Fig. 4** online).

Coupled Grx1 mediates a glutathione-specific sensor response

Previous studies have shown that glutaredoxins selectively interact with glutathione and discriminate against other redox-active compounds[19]. To confirm that Grx1 confers glutathione specificity to the biosensor, we evaluated its *in vitro* response to reduction by ascorbate or cysteine and to oxidation by cystine or hydroxyethyl disulfide. As expected, only incubation with glutathione led to a substantial sensor response (**Supplementary Fig. 5** online). Thus, the previously described specificity of Grx1 for glutathione is also given in the context of the Grx1-roGFP2 fusion protein.

Notably, the presence of micromolar H_2O_2 by itself did not lead to substantial sensor oxidation within the measurement period. Instead, H_2O_2-mediated sensor oxidation depended on the concomitant presence of glutathione (**Fig. 1e**). Catalytic amounts of glutathione peroxidase further enhanced the sensor response to H_2O_2 (**Fig. 1e**), thus confirming that glutathione oxidation precedes and facilitates sensor oxidation.

Grx1-roGFP2 does not engage in disulfide exchange with Trx1

Although fusion of Trx1 did not influence the response of roGFP2 to glutathione (**Fig. 1a**), we considered the possibility that Trx1 might be able to directly reduce oxidized roGFP2 or Grx1-roGFP2. When we exposed fully oxidized Grx1-roGFP2 to the complete thioredoxin system, we observed only slight sensor responses (**Supplementary Fig. 6** online). This finding demonstrated that the engineered disulfide bond of roGFP2 is not efficiently targeted by Trx1 and suggested that the Trx system is unlikely to interfere with Grx1-roGFP2 redox behavior.

Grx1-roGFP2 facilitates imaging of intracellular redox changes

To investigate the redox-sensing properties of Grx1-roGFP2 in living cells, we stably expressed Grx1-roGFP2 and roGFP2 in HeLa cells. We treated cells with a single bolus of 50 μM H_2O_2, followed 2 min later by exposure to 0.5 mM dithiothreitol (DTT). Addition of H_2O_2 to the growth medium led to an immediate and strong oxidative response in Grx1-roGFP2-positive cells (**Fig. 2a**). The sensor remained in the oxidized state until injection of DTT induced its reduction. In contrast, uncoupled roGFP2 responded

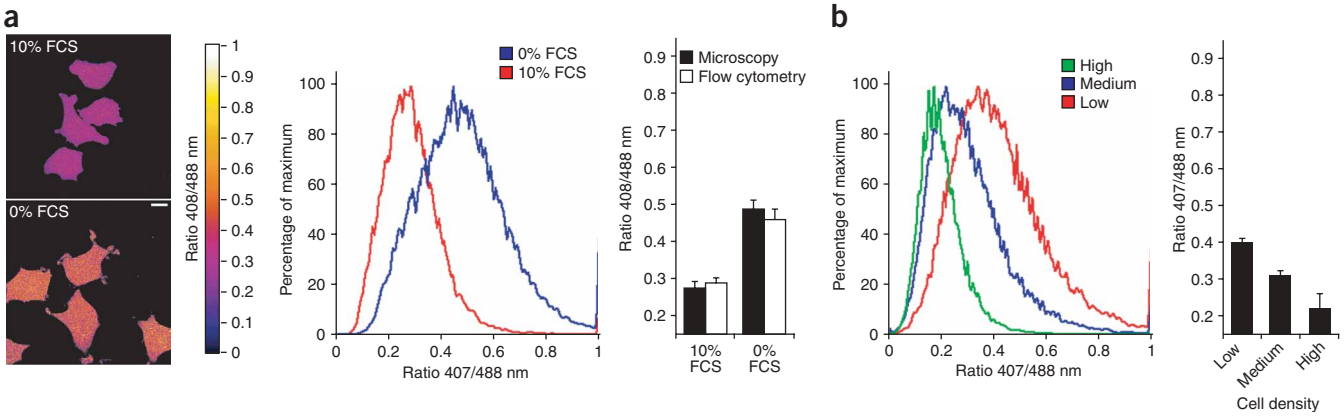

Figure 3 | Redox response of HeLa cells to growth-factor starvation and changes in cell density. (**a**) HeLa cells expressing Grx1-roGFP2 were incubated in medium containing 0 or 10% FCS for 20 h and analyzed by microscopy (left; scale bar, 10 μm) and flow cytometry (middle). For quantification of microscopy data, emission ratios from 12 cells in 3 different experiments were averaged. Both techniques revealed similar results (right). (**b**) Grx1-roGFP2-expressing HeLa cells seeded at different densities (average cell density: low, 1.6×10^4; medium, 4×10^4; and high, 8×10^4 cells/cm^2) were analyzed by flow cytometry after 24 h (left). We analyzed 30,000 cells from three different experiments, and the average of the mean ratio was calculated (right). Error bars represent s.d. from the mean. Data are representative of three experiments.

slowly and did not reach the same oxidation level within the given timeframe. We obtained similar results with various transiently transfected cell lines (data not shown).

To estimate the sensitivity of the Grx1-roGFP2 sensor protein, we tested its response to exogenously added H_2O_2. Addition of H_2O_2 in the low-micromolar range led to short-lived deflections of E_{GSH} lasting 90–120 s, suggestive of an efficient anti-oxidative response (**Fig. 2b**). Accordingly, addition of larger amounts of H_2O_2 led to increased and prolonged shifts of E_{GSH} (**Fig. 2b**). Addition of extracellular H_2O_2 in the low micromolar range, likely leading to nanomolar concentrations of intracellular GSSG[20,21], was sufficient to elicit a sensor response (**Fig. 2c**). A response to limiting amounts of H_2O_2 was barely detectable in cells with unfused roGFP2 (**Supplementary Fig. 7** online), thus confirming that slow equilibration impedes the detection of short-lived oxidative events by roGFP2.

Redox changes caused by growth conditions

We then asked whether the fusion protein would allow detection of endogenous redox changes. Previously, it has been shown that growth factor deprivation causes an increase in intracellular ROS[22]. We cultured Grx1-roGFP2–expressing HeLa cells in the presence

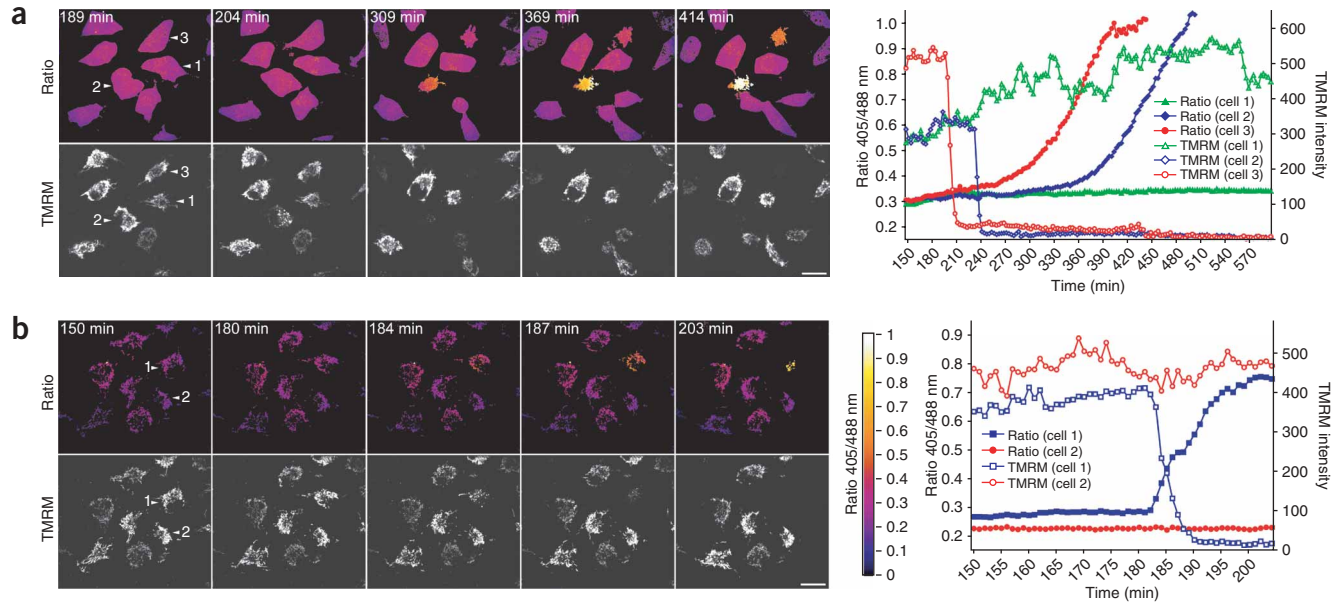

Figure 4 | Grx1-roGFP2 visualizes redox changes associated with TRAIL-induced apoptosis. (**a**) Apoptosis was induced in Grx1-roGFP2–expressing HeLa cells by the addition of 400 ng/ml TRAIL. $\Delta\Psi$ was visualized with TMRM. False-color ratio and TMRM intensity images at different time points are depicted (left). Cell 1 maintained $\Delta\Psi$ during the measurement period whereas cells 2 and 3 responded to the TRAIL treatment (arrowheads). The emission ratio of Grx1-roGFP2 (excitation lines 405 and 488 nm) and the TMRM intensity for the selected cells were plotted against time (right). (**b**) A mitochondrial-targeted Grx1-roGFP2 was used in experiments similar to **a**. False-color ratio and TMRM intensity pictures (left) as well as quantification diagrams (right) are shown for a responding (arrowhead 1) and a non-responding cell (arrowhead 2). Scale bars, 20 μm. Data are representative of five (**a**) or three (**b**) experiments.

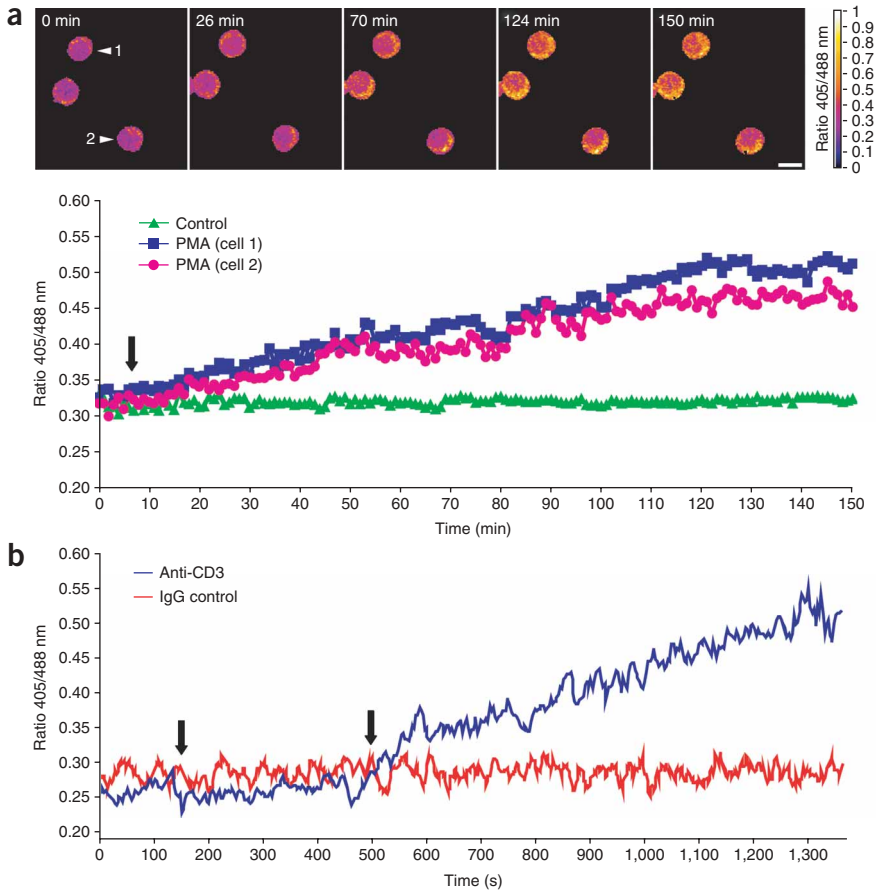

Figure 5 | Grx1-roGFP2 visualizes physiological redox changes associated with immune-cell activation. (**a**) Grx1-roGFP2–positive mouse RAW264.7 cells were stimulated with 1 μM PMA after 6 min. False-color ratio pictures of PMA-treated cells are depicted at representative time points (top). Scale bar, 10 μm. The sensor ratio of two stimulated cells (arrowheads) and one control cell was calculated and plotted over time (bottom). (**b**) Isolated primary human T cells were transiently transfected with Grx1-roGFP2 and analyzed by time-resolved flow cytometry. After 150 s (left arrow), cells were subjected to either anti-CD3 or isotype control antibody for another 350 s. Cross-linking of primary antibody was then induced by injection of goat-anti-mouse antibody (right arrow). The emission ratio (excitation wavelengths 405 and 488 nm) was plotted against time. Data from approximately 40–60 cells were averaged per second. Data are representative of three experiments.

or absence of serum and determined E_{GSH} by microscopy and flow cytometry (**Fig. 3a**). To analyze the distribution of redox potential in cell populations by flow cytometry, we made use of the fact that the thiol-disulfide status of the biosensor can be 'clamped' by a brief treatment of intact cells with the membrane-permeable alkylating agent *N*-ethyl maleimide (NEM), thus allowing for fixation and additional handling without impairing sensor redox status (**Supplementary Fig. 8** online). Both techniques revealed very similar ratiometric changes (**Fig. 3a**), corresponding to an oxidative shift in E_{GSH} approximately from –300 to –280 mV. We independently confirmed an increase in endogenous ROS in the same cells using the redox-sensitive dye 2′,7′-dichlorodihydrofluorescein diacetate (H_2DCFDA; **Supplementary Fig. 9** online).

It has also been suggested that endogenous oxidant levels depend on cell density[23]. To determine whether intracellular E_{GSH} is influenced by cell density, we seeded Grx1-roGFP2–expressing HeLa cells at different densities, allowed them to adhere in fresh medium and analyzed them by flow cytometry. We observed a reproducible correlation between redox state and cell density; greater cell density led to more reduced E_{GSH} (**Fig. 3b**). A fivefold increase in cell density decreased E_{GSH} by approximately 40 mV, from –280 to –320 mV. The change in E_{GSH} correlated with corresponding changes in the amount of endogenous ROS, as confirmed by H_2DCFDA staining (**Supplementary Fig. 9**).

Endogenous redox changes associated with apoptosis

Apoptosis is known to be associated with oxidative redox changes, caused by mitochondrial ROS production and, possibly, active extrusion of reduced glutathione[4,24,25]. Redox changes inside mitochondria are connected to the permeability transition, a critical control point in apoptosis[26]. We followed E_{GSH} during apoptosis in both the cytosolic and mitochondrial compartments. To this end, we targeted the Grx1-roGFP2 fusion protein to the mitochondrial matrix using a signal sequence from *Neurospora crassa* ATP synthase protein 9 ('mito-Grx1-roGFP2'). We treated sensor-expressing cells with TNF-related apoptosis-inducing ligand (TRAIL) to induce apoptosis, using a concentration that led to 60% cell death within 16 h. Additionally, we loaded the cells with tetramethylrhodamine methyl ester (TMRM) to monitor the mitochondrial membrane potential ($\Delta\Psi$). As this dye may produce ROS upon strong illumination[27], we chose very mild exposition conditions to minimize this effect. Between 2 and 5 h after addition of TRAIL, individual cells lost $\Delta\Psi$. Mitochondrial depolarization typically occurred over 10–15 min. The cytosolic E_{GSH} remained stable before the loss of $\Delta\Psi$. Following loss of $\Delta\Psi$ and an additional delay of 15–20 min, cytosolic E_{GSH} increased continuously over the next 3–4 h, from a ground state potential of approximately –290 mV to >–240 mV, thus reaching sensor saturation (**Fig. 4a**). Control experiments testing Sytox orange uptake confirmed that the plasma membrane remained intact during the measurement period and that loss of cellular integrity led to an overall loss of sensor signal without measurable sensor oxidation (data not shown). The observed changes in $\Delta\Psi$ and E_{GSH} did not occur in the absence of TRAIL treatment (data not shown). In contrast to the observations in the cytoplasm, the increase in glutathione oxidation inside mitochondria occurred concurrently with the decrease of $\Delta\Psi$, and maximal oxidation was reached within 15 min (**Fig. 4b**). Thus it appeared that mitochondrial glutathione oxidation is directly coupled to the drop in $\Delta\Psi$, whereas oxidation of the cytosolic glutathione pool followed with a temporal delay.

Oxidant formation mediated by NADPH oxidase

The generation of oxidants by phagocyte NADPH oxidase (Phox) is one important cellular defense against pathogens upon first

contact. *In vitro*, Phox-mediated oxidant formation can be induced by phorbol ester[28]. Treatment of biosensor-expressing RAW264.7 macrophages with phorbol 12-myristate 13-acetate (PMA) during live-cell imaging demonstrated a continuous increase in cytosolic oxidation, which leveled after approximately 2 h (**Fig. 5a**). We confirmed the oxidative response in the same experiment by H_2DCFDA staining (**Supplementary Fig. 10** online).

Oxidant formation induced by T-cell receptor stimulation

T-cell receptor stimulation is known to induce rapid cytosolic oxidant generation[29], and H_2O_2 has been found to function as an essential second messenger in T-cell receptor signaling[30]. To clarify whether the Grx1-roGFP2 biosensor allows the detection of a rapid receptor-triggered ROS signal, we transiently transfected primary peripheral human T cells with the biosensor and used time-resolved flow cytometry to follow the cytosolic redox state. T-cell stimulation through cross-linking of T-cell receptors led to a substantial increase in cytosolic oxidation, reaching approximately 75% sensor oxidation within 10 min (**Fig. 5b**). Addition of soluble antibodies to CD3 alone or cross-linking of isotype-matched control antibodies did not induce an oxidative response.

DISCUSSION

Ideally, redox sensors should be non-disruptive, dynamic, sensitive and specific for a defined redox pair of interest. The genetically encoded redox biosensor reported here is based on the ability of roGFP2 to mimic a natural Grx1 target protein in that it becomes dynamically oxidized and reduced in response to E_{GSH}, comparable to physiological Grx1 target proteins[31]. The relevance of this concept is also emphasized by our recent observation that roGFP2 expressed in *Arabidopsis thaliana* specifically responds to the cytosolic glutathione redox buffer, a response most likely mediated by plant glutaredoxins, which are far more abundant than their counterparts in animal cells[32]. Moreover, quantitative analysis of roGFP2 fluorescence in *Arabidopsis* mutants partially deficient in glutathione biosynthesis confirmed that measured changes in E_{GSH} are consistent with theoretical predictions derived from the Nernst equation[32].

The operating mode of Grx1-roGFP2 appears to rest upon the established monothiol mechanism of Grx1, as removal of the second thiol in the active site (Cys26) did not notably change the redox-sensing behavior of Grx1-roGFP2 in live-cell experiments (data not shown). Nucleophilic Cys23 is known to interact with GSSG to form a mixed protein-glutathione disulfide intermediate. According to the reaction mechanism of glutaredoxins[33,34], subsequent oxidation of roGFP2 is likely mediated via glutathionylation of one of the two roGFP2 cysteines. This notion is also supported by the absence of detectable mixed disulfide intermediates between Grx1 and roGFP2 (data not shown).

Our observations are in line with a recent *in vitro* study using the fusion of yeast glutaredoxin-1 (Grx1p) to redox-sensitive yellow fluorescent protein (rxYFP) to obtain mechanistic insight into the enzymatic mechanism of glutaredoxin[35]. However, the rxYFP-Grx1p fusion protein differs from Grx1-roGFP2 in ways that appear to limit its use as a biosensor: rxYFP does not show ratiometric behavior, and its dithiol-disulfide pair is less negative in mid-point potential (–265 mV), thus making it less responsive to small changes in glutathione oxidation.

Responding to low-micromolar concentrations of exogenously added H_2O_2, Grx1-roGFP2 in HeLa cells was no less sensitive than HyPer under comparable conditions[15], although the latter is a dedicated H_2O_2 sensor, directly oxidized by H_2O_2. In contrast to HyPer, the intracellular response of Grx1-roGFP2 to low amounts of H_2O_2 depends on the formation of GSSG, likely mediated by endogenous glutathione peroxidases. Of note, the maximal ratiometric change for HyPer in living cells is about 2.4, as compared to a more favorable factor of 4.4 for Grx1-roGFP2. Another difference between Grx1-roGFP2 and HyPer is that the redox state of the former is driven in both directions by the same redox pair (GSH and GSSG), whereas the redox state of the latter represents the interplay between H_2O_2-mediated oxidation and an intracellular reducing system.

The expression of Grx1-roGFP2 allowed observation of the real-time response of the intracellular glutathione system to exogenously applied agents. In principle, such measurements can be applied to any compound—for example, antioxidants or xenobiotics—thus suggesting applications in drug screening and toxicology. Expression of Grx1-roGFP2 also permitted the measurement of endogenous redox changes, including those associated with growth-factor deprivation, cell density and apoptosis. Similar to HyPer[15], Grx1-roGFP2 revealed a close relationship between $\Delta\Psi$ and the mitochondrial redox state. By targeting one version of Grx1-roGFP2 to the mitochondrial matrix, we resolved the temporal delay between mitochondrial and cytoplasmic glutathione oxidation. Finally, the detection of a receptor-triggered ROS signal in primary human lymphocytes suggests that the Grx1-roGFP2 biosensor affords the observation of physiological redox signals similar to those that would be experienced by cells *in vivo* under normal circumstances.

METHODS

***In vitro* measurements of the roGFP2 redox state.** We expressed recombinant proteins (Grx1-roGFP2, Grx1(SS)-roGFP2, Trx1-roGFP2, roGFP2 and Trx1) in *Escherichia coli* strains BL21 (Stratagene) or M15 (Qiagen) and purified via hexahistidine affinity chromatography. The purified recombinant proteins were desalted (Slide-A-Lyzer dialysis cassettes; Pierce) and diluted into a standard reaction buffer (100 mM potassium phosphate, 1 mM EDTA; pH 7.0) to a final concentration of 1 μM. We measured the emission of roGFP2 (505–515 nm) after excitation at 390 and 480 nm in a plate reader (FLUOstar Optima; BMG Labtech) equipped with built-in injectors. We calculated the ratio of the emission (390/480 nm) and plotted it against time. For better comparability, we set the ratio of fully reduced protein to 0.1. For oxidation experiments, we first reduced the proteins with 20 mM DTT for 20 min on ice and desalted them with Zeba Desalt spin columns (Pierce).

Cell culture and imaging of living cells. We grew HeLa and RAW264.7 cells in DMEM (Gibco) supplemented with 10% heat-inactivated FBS, 2 mM L-glutamine, 100 U/ml penicillin and 100 μg/ml streptomycin (Gibco). We generated HeLa cells stably expressing Grx1-roGFP2 or roGFP2 by retroviral transduction and subsequent selection with 0.5 μg/ml puromycin. We created Grx1-roGFP2–expressing RAW264.7 cells by lentiviral infection. To monitor $\Delta\Psi$, we loaded HeLa cells expressing Grx1-roGFP2 with 30 nM TMRM (Molecular Probes). Apoptosis was induced by addition of 400 ng/ml of TRAIL. We monitored membrane integrity by staining with 50 nM Sytox orange (Molecular Probes).

We seeded cells and imaged them in FD-35 FluoroDishes (World Precision Instruments), and the temperature was maintained at 37 °C by a stage top incubator (Tokai Hit) mounted on a Nikon Te2000 inverted microscope. We used either a Nikon C1Si confocal laser scanning microscope or a Perkin ElmerUltra View ERS spinning disk confocal system with similar results. The Nikon C1Si confocal laser scanning system on a TE2000 E was equipped with a PlanApo VC 60×, 1.2 numerical aperture (NA) objective (water immersion). We excited the biosensor sequentially frame by frame with the 408 nm and 488 nm laser line and detection set to 500–530 nm. The Perkin Elmer Ultra View ERS spinning disk confocal microscope on a Nikon TE2000 U was equipped with a PlanApo VC 60×, 1.4 NA objective (oil immersion). For RAW264.7 cells we used a PlanApo VC 60×, 1.2 NA objective (water immersion). We excited Grx1-roGFP2 by the 405 nm and 488 nm laser line and detected the emission through a 500–554 nm bandpass filter on an electron-multiplying charge-coupled device (EM-CCD; C9100-02; Hamamatsu). We visualized TMRM by excitation at 568 nm and detected with a 580–650 nm emission filter. Raw data were exported to ImageJ software (http://rsb.info.nih.gov/ij/) as 16-bit TIF for analysis. We subtracted background of the images and set a threshold to avoid ratio-created artifacts. We created ratio images by dividing the 405/408 nm picture by the 488 nm image pixel by pixel. We used the ImageJ look up table 'Fire' for creating false-color ratio pictures.

Additional methods. Descriptions of cloning of biosensor expression constructs, calculation of redox potentials, flow cytometry of biosensor-expressing HeLa cells, and the isolation, transfection and flow cytometry of primary T cells are available in **Supplementary Methods**.

Note: Supplementary information is available on the Nature Methods website.

ACKNOWLEDGMENTS

We thank J. Remington (University of Oregon) for providing the roGFP2 construct; M. Winkler, S. Hoffmann and E. Sollner for technical assistance; H. Walczak (German Cancer Research Center) for TRAIL protein; U. Engel and C. Ackermann (Nikon Imaging Center at the University of Heidelberg) for providing microscope access and assistance. Supported by the European Commission (Marie Curie Excellence Grant 2761 'Redox signaling' to T.P.D.).

1. Dröge, W. Free radicals in the physiological control of cell function. *Physiol. Rev.* **82**, 47–95 (2002).
2. Menon, S.G. & Goswami, P.C. A redox cycle within the cell cycle: ring in the old with the new. *Oncogene* **26**, 1101–1109 (2007).
3. Balaban, R.S., Nemoto, S. & Finkel, T. Mitochondria, oxidants, and aging. *Cell* **120**, 483–495 (2005).
4. Filomeni, G. & Ciriolo, M.R. Redox control of apoptosis: an update. *Antioxid. Redox Signal.* **8**, 2187–2192 (2006).
5. Veal, E.A., Day, A.M. & Morgan, B.A. Hydrogen peroxide sensing and signaling. *Mol. Cell* **26**, 1–14 (2007).
6. Ramsey, M.R. & Sharpless, N.E. ROS as a tumour suppressor? *Nat. Cell Biol.* **8**, 1213–1215 (2006).
7. Colavitti, R. & Finkel, T. Reactive oxygen species as mediators of cellular senescence. *IUBMB Life* **57**, 277–281 (2005).
8. Lambeth, J.D. NOX enzymes and the biology of reactive oxygen. *Nat. Rev. Immunol.* **4**, 181–189 (2004).
9. Houstis, N., Rosen, E.D. & Lander, E.S. Reactive oxygen species have a causal role in multiple forms of insulin resistance. *Nature* **440**, 944–948 (2006).
10. Jones, D.P. Redefining oxidative stress. *Antioxid. Redox Signal.* **8**, 1865–1879 (2006).
11. Trotter, E.W. & Grant, C.M. Overlapping roles of the cytoplasmic and mitochondrial redox regulatory systems in the yeast *Saccharomyces cerevisiae*. *Eukaryot. Cell* **4**, 392–400 (2005).
12. Hansen, J.M., Go, Y.M. & Jones, D.P. Nuclear and mitochondrial compartmentation of oxidative stress and redox signaling. *Annu. Rev. Pharmacol. Toxicol.* **46**, 215–234 (2006).
13. Pani, G. *et al.* Cell compartmentalization in redox signaling. *IUBMB Life* **52**, 7–16 (2001).
14. Rota, C., Chignell, C.F. & Mason, R.P. Evidence for free radical formation during the oxidation of 2'-7'-dichlorofluorescin to the fluorescent dye 2'-7'-dichlorofluorescein by horseradish peroxidase: possible implications for oxidative stress measurements. *Free Radic. Biol. Med.* **27**, 873–881 (1999).
15. Belousov, V.V. *et al.* Genetically encoded fluorescent indicator for intracellular hydrogen peroxide. *Nat. Methods* **3**, 281–286 (2006).
16. Ostergaard, H., Henriksen, A., Hansen, F.G. & Winther, J.R. Shedding light on disulfide bond formation: engineering a redox switch in green fluorescent protein. *EMBO J.* **20**, 5853–5862 (2001).
17. Hanson, G.T. *et al.* Investigating mitochondrial redox potential with redox-sensitive green fluorescent protein indicators. *J. Biol. Chem.* **279**, 13044–13053 (2004).
18. Dooley, C.T. *et al.* Imaging dynamic redox changes in mammalian cells with green fluorescent protein indicators. *J. Biol. Chem.* **279**, 22284–22293 (2004).
19. Gravina, S.A. & Mieyal, J.J. Thioltransferase is a specific glutathionyl mixed disulfide oxidoreductase. *Biochemistry* **32**, 3368–3376 (1993).
20. Antunes, F. & Cadenas, E. Estimation of H_2O_2 gradients across biomembranes. *FEBS Lett.* **475**, 121–126 (2000).
21. Winterbourn, C.C. & Metodiewa, D. Reactivity of biologically important thiol compounds with superoxide and hydrogen peroxide. *Free Radic. Biol. Med.* **27**, 322–328 (1999).
22. Satoh, T., Sakai, N., Enokido, Y., Uchiyama, Y. & Hatanaka, H. Survival factor-insensitive generation of reactive oxygen species induced by serum deprivation in neuronal cells. *Brain Res.* **733**, 9–14 (1996).
23. Pani, G. *et al.* A redox signaling mechanism for density-dependent inhibition of cell growth. *J. Biol. Chem.* **275**, 38891–38899 (2000).
24. Franco, R. & Cidlowski, J.A. SLCO/OATP-like transport of glutathione in FasL-induced apoptosis: glutathione efflux is coupled to an organic anion exchange and is necessary for the progression of the execution phase of apoptosis. *J. Biol. Chem.* **281**, 29542–29557 (2006).
25. Danial, N.N. & Korsmeyer, S.J. Cell death: critical control points. *Cell* **116**, 205–219 (2004).
26. Ferri, K.F. & Kroemer, G. Mitochondria–the suicide organelles. *Bioessays* **23**, 111–115 (2001).
27. Zorov, D.B., Filburn, C.R., Klotz, L.O., Zweier, J.L. & Sollott, S.J. Reactive oxygen species (ROS)-induced ROS release: a new phenomenon accompanying induction of the mitochondrial permeability transition in cardiac myocytes. *J. Exp. Med.* **192**, 1001–1014 (2000).
28. Green, S.P. & Phillips, W.A. Activation of the macrophage respiratory burst by phorbol myristate acetate: evidence for both tyrosine-kinase-dependent and -independent pathways. *Biochim. Biophys. Acta* **1222**, 241–248 (1994).
29. Jackson, S.H., Devadas, S., Kwon, J., Pinto, L.A. & Williams, M.S. T cells express a phagocyte-type NADPH oxidase that is activated after T cell receptor stimulation. *Nat. Immunol.* **5**, 818–827 (2004).
30. Gulow, K. *et al.* HIV-1 trans-activator of transcription substitutes for oxidative signaling in activation-induced T cell death. *J. Immunol.* **174**, 5249–5260 (2005).
31. Ghezzi, P. Regulation of protein function by glutathionylation. *Free Radic. Res.* **39**, 573–580 (2005).
32. Meyer, A.J. *et al.* Redox-sensitive GFP in *Arabidopsis thaliana* is a quantitative biosensor for the redox potential of the cellular glutathione redox buffer. *Plant J.* **52**, 973–986 (2007).
33. Peltoniemi, M.J., Karala, A.R., Jurvansuu, J.K., Kinnula, V.L. & Ruddock, L.W. Insights into deglutathionylation reactions: different intermediates in the glutaredoxin and protein disulphide isomerase catalysed reactions are defined by the gamma-linkage present in glutathione *J. Biol. Chem.* **281**, 33107–33114 (2006).
34. Fernandes, A.P. & Holmgren, A. Glutaredoxins: glutathione-dependent redox enzymes with functions far beyond a simple thioredoxin backup system. *Antioxid. Redox Signal.* **6**, 63–74 (2004).
35. Björnberg, O., Østergaard, H. & Winther, J.R. Mechanistic insight provided by glutaredoxin within a fusion to redox-sensitive yellow fluorescent protein. *Biochemistry* **45**, 2362–2371 (2006).